AIP | Conference Proceedings

Algorithms for Ultrasonic Spacecraft Leak Location Using Structure Borne Noise

Stephen D. Holland, Ron Roberts, D. E. Chimenti, and Michael Strei

Citation: AIP Conf. Proc. **760**, 1107 (2005); doi: 10.1063/1.1916796
View online: http://dx.doi.org/10.1063/1.1916796
View Table of Contents: http://proceedings.aip.org/dbt/dbt.jsp?KEY=APCPCS&Volume=760&Issue=1
Published by the American Institute of Physics.

ALGORITHMS FOR ULTRASONIC SPACECRAFT LEAK LOCATION USING STRUCTURE BORNE NOISE

Stephen D. Holland[1], Ron Roberts[1], D. E. Chimenti[2], and Michael Strei[1]
[1]Center for NDE, Iowa State Univ, Ames, Iowa 50011
[2]Center for NDE and Aerospace Eng Dept, Iowa State Univ, Ames, Iowa 50011

ABSTRACT. Micrometeorite induced air leaks pose a substantial danger to manned spacecraft. An algorithm for identifying and locating air leaks in spacecraft by monitoring cross-correlations of leak-generated guided ultrasonic waves in the spacecraft's plate-like skin using a minimal array of sensors is described, The algorithm utilizes a-priori knowledge of guided-mode dispersion to invert that dispersion and thereby identify possible location curves for the leak source. The intersection of curves from multiple correlations identifies a specific location for the leak source.

INTRODUCTION

All manned space vehicles are vulnerable to damage by hits from micrometeorites and space debris. Because of the huge kinetic energies involved, even tiny particles can cause serious damage; a 1-mm particle impact to a space shuttle wing leading edge may be sufficient to cause loss-of-vehicle during reentry [1], yet only 10 cm and larger debris can be tracked by radar and avoided [2]. Should such a debris hit penetrate the shielding and pressure vessel of a manned spacecraft, the air leak could be plugged if the leak can be found quickly enough before scarce air can escape. In this paper, we discuss methods and algorithms for finding the location of such a leak with data from sensors embedded within the structure of the spacecraft.

METHOD

Figure 1 illustrates the generation of ultrasonic noise by a leak into vacuum. Energy from the leak couples into Rayleigh-Lamb guided ultrasonic waves that propagate through the

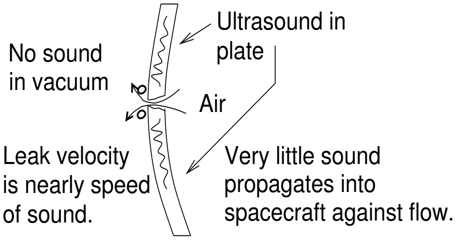

FIGURE 1. Diagram showing air leaking out of a spacecraft (right) to a vacuum (left) and showing sound generated in the spacecraft skin

CP760, *Review of Quantitative Nondestructive Evaluation Vol. 24,* ed. by D. O. Thompson and D. E. Chimenti

FIGURE 2. Correlation transforms noise waveforms into predictable functions of the leak spectrum and geometry.

FIGURE 3. Example measured cross-correlation.

structure away from the source of the leak. This ultrasound can be detected by point sensors attached to the spacecraft skin. Unfortunately, the leak noise can be so faint that it is buried in noise from other sources. By cross-correlating [3] the measured waveforms from two sensors, those waveforms can be transformed from random noise into a predictable function of the leak spectrum and the geometry. Figure 2 illustrates why this is the case. If we represent a single-frequency component of the leak noise by $\tilde{\mathrm{A}}e^{j\omega t}$, with its randomness represented by the complex phase of $\tilde{\mathrm{A}}$, then the measured waveform at a distance d will be that same waveform, phase delayed according to the distance (and also attenuated in amplitude, but this is irrelevant to the analysis):

$$\tilde{\mathrm{A}}e^{j\omega t - jkd} \tag{1}$$

The cross-correlation of two of these waveforms at distances d_1 and d_2 is

$$\tilde{\mathrm{A}}^*\tilde{\mathrm{A}}e^{jk(d_1-d_2)}e^{j\omega t}. \tag{2}$$

Because the product of $\tilde{\mathrm{A}}$ with its complex conjugate is real, the cross-correlation is not random, but a predictable function of the leak spectrum and the geometry. With a sufficiently long correlation, spurious noise will average to zero and large signal-to-noise ratios can be obtained for the leak. Figure 3 shows an example measured correlation from a one-second acquisition.

The analysis of measured correlations of leak noise is complicated by the existence of multiple guided Lamb modes that can propagate in the structure, by interference between

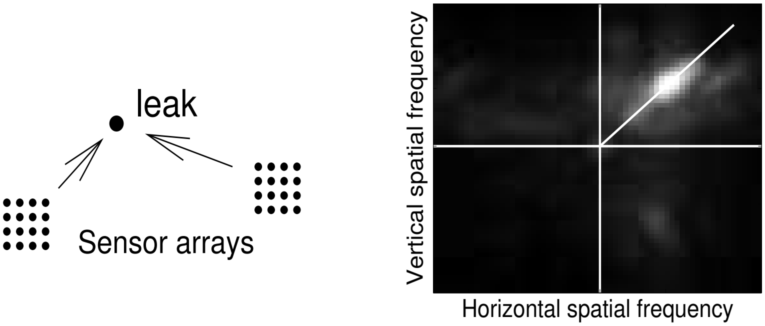

(a) (b)

FIGURE 4. (a) Diagram of the phased array leak location method. (b) Two dimensional spatial Fourier transform of measured array data indicating direction to the leak.

these modes, by the dispersive nature of these modes, and by the presence of echos and resonances between edges. One algorithm that is unaffected by dispersion and multimode propagation is the phased array/synthetic aperture method. This method involves using a pair of sensor arrays, illustrated in Fig. 4a. All possible correlations between a single reference sensor and the elements of an array are recorded. The measured correlations are then spatially Fourier transformed in x and y to give a 2-dimensional mapping of the leak energy in spatial wavenumber space. Figure 4b shows a measured mapping from a 256 element scanned array. The direction from the array to the leak is then obvious (45° in Fig. 4), and the process can be repeated with a second array to locate the leak precisely through triangulation. While this method is ideal in that it is inherently insensitive to interference, it has the limitation of requiring large 2D sensor arrays and substantial computation to compute the correlations. For this reason, the phased array method is not yet practical. In this paper, we will focus on an alternative algorithm that relies on only a few scattered individual transducers to identify the leak location.

This alternative algorithm involves comparing the measured cross-correlations from pairs of these scattered transducers with simulated correlations calculated assuming a particular location for the leak, thereby determining a perceived source strength for the leak at that location. By exhaustively comparing the measured correlations with correlations calculated assuming all possible leak locations, the leak location can be determined. In our tests, four narrow-aperture piezoelectric transducers are distributed over a 24-inch square aluminum plate, 3/16-inch thick. A 1-mm hole has been drilled in the plate and the area behind the hole has been evacuated.

Simulated correlations for the comparison are calculated by taking an assumed flat frequency spectrum of a single mode and setting the phase at each frequency according to Eq. 2 from the difference in propagation distances from the assumed leak location to the two transducers. The perceived source strength for that mode and leak location from those transducers is then the magnitude of the inner product over a limited frequency band between the simulated and measured correlations. Source strength maps from each correlation and each mode are then combined to yield a composite map. This process is illustrated in Fig. 5. Figure 5a shows a source strength map from the measured correlation from the two rightmost transducers (marked with circles) assuming propagation in the A_0 Lamb mode. Fig. 5b shows the same waveform, processed instead assuming propagation in the S_0 Lamb mode. Fig. 5c shows a source strength map assuming A_0 propagation from another transducer pair, and Fig. 5d shows that same correlation analyzed assuming S_0 propagation. To create the

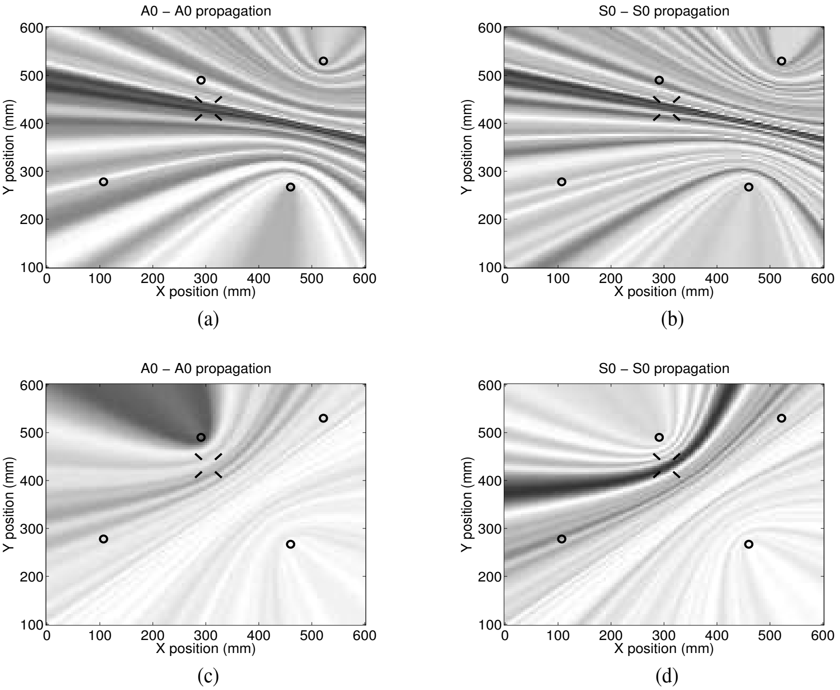

FIGURE 5. (a) Source strength map for transducer pair #1, assuming A_0 propagation. (b) Source strength map for transducer pair #1, assuming S_0 propagation. (c) Source strength map for transducer pair #2, assuming A_0 propagation. (d) Source strength map for transducer pair #2, assuming S_0 propagation.

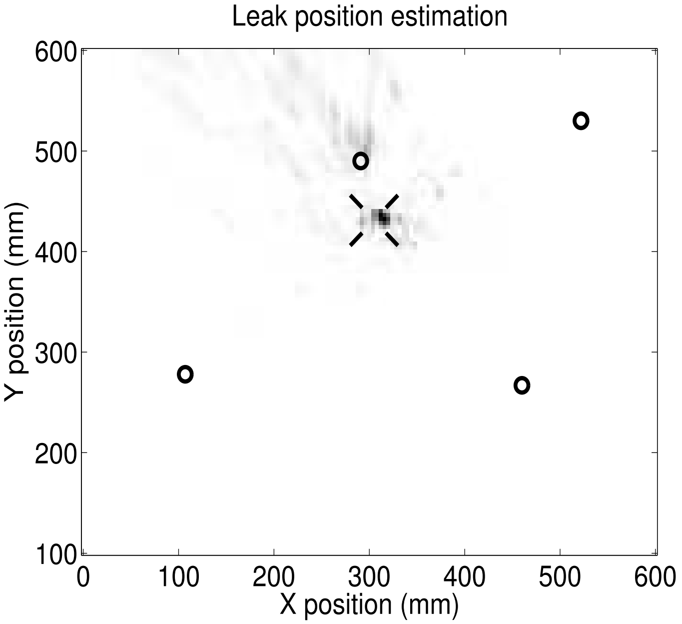

FIGURE 6. Composite source strength map.

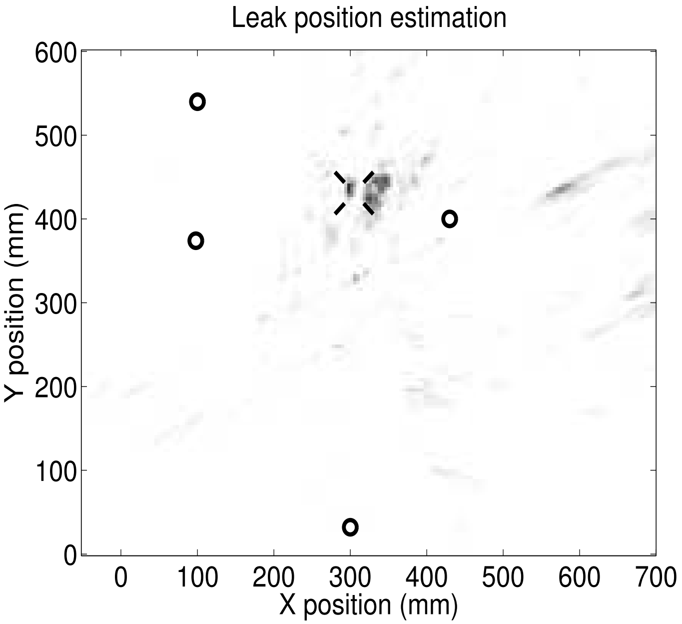

FIGURE 7. Composite source strength map from a different sensor configuration.

composite source strength map, the maps from six all possible correlations assuming A_0 propagation are multiplied together, and that product is added to the product of the six maps assuming S_0 propagation. The composite image is the sum of those products. Figure 6 shows the composite image, the product of Figs. 5a, 5c, and the other A_0 maps added to the product of Figs. 5b, 5d, and the other S_0 maps. The peak in Fig. 6 is but a few mm from the actual location of the leak. Likewise, Fig. 7 shows a leak location map from a different transducer configuration, again with the peak very close to the actual leak location.

CONCLUSIONS

The algorithm described above transforms cross-correlations between measured waveforms into a map of possible leak locations. It exploits *a priori* knowledge of the material properties and the dispersion of Lamb modes. It analyzes the measured correlations independently for each mode, assuming no other modes are present, and because of interference and misidentification it may possibly predict multiple candidate leak locations. Nevertheless we have demonstrated that this algorithm can accurately identify the location of a 1-mm leak-into-vacuum from just six recorded cross-correlations from four sensors in 3/16-inch aluminum.

ACKNOWLEDGMENTS

This material is based on work supported by NASA under award NAG-1-029098.

REFERENCES

1. Committee on Space Shuttle Meteoroid/Debris Risk Management, National Research Council, Protecting the Space Shuttle from Meteoroids and Orbital Debris, (The National Academies Press, Washington D.C. 1997).
2. L. Foster, J. Frisbee, M. Wortham, and L. Howorth, The Orbital Debris Quarterly News 6(2) 4-5 (2001)
3. M. Strei, R. Roberts, S. Holland, and D. E. Chimenti, “Leak location in plates: compensation for multimode dispersion”, in *Review of Progress in QNDE*, Vol. 23B, eds. D. O. Thompson and D. E. Chimenti, (AIP Press, New York) 2003, pp 1398–1405.